Food Research International 128 (2020) 108746

Contents lists available at ScienceDirect

Food Research International

journal homepage: www.elsevier.com/locate/foodres

The stabilizing effect of cellulose crystals in O/W emulsions obtained by ultrasound process

Aureliano Agostinho Dias Meirelles, Ana Letícia Rodrigues Costa, Rosiane Lopes Cunha*

School of Food Engineering, University of Campinas, Rua Monteiro Lobato, 80, 13083-862 Campinas, SP, Brazil

ARTICLE INFO

Keywords:
Cellulose crystal
Stability of emulsion
Flaxseed oil
Ultrasound processing

ABSTRACT

The encapsulation of lipophilic bioactive compounds, such as flaxseed oil, is usually done using O/W emulsions as carrier matrix. The aim of this study was to understand the stabilization mechanism of micro-nano cellulose crystals produced from acid hydrolysis in O/W emulsion. Effects of emulsification process conditions using ultrasound on the cellulose particles properties were evaluated varying the proportion of oil-cellulose particles in the emulsion formulation. Cellulose structure did not change using different conditions of emulsification and X-ray diffraction showed major presence of cellulose I. Particle size distribution of cellulose was bimodal and mean particle size reduced after hydrolysis. Emulsions stabilized by cellulose were opaque, homogeneous and showed good kinetic stability. The largest microcrystals were displayed between the oil droplets, preventing the flocculation of the droplets while smaller particles were adsorbed on the oil-water interface. The mechanism of droplets stabilization was not associated to the reduction of interfacial tension. Stabilization was associated to significant effect of electrostatic repulsion and increase in viscosity. Moreover, the flaxseed oil droplets were completely surrounded by cellulose nanocrystals, showing also Pickering-type stabilization. Therefore, emulsions with cellulose crystals were stabilized by different mechanisms and have interesting properties and characteristics for the protection of lipophilic compounds that could be applied in food and cosmetics products.

1. Introduction

Pharmaceutical, cosmetics and food industries have increased investments to replace synthetic additives by natural compounds meeting expectations of an increasingly demanding consumer for related health care (Piorkowski & McClements, 2013). In this way the encapsulation of bioactive compounds is relevant to increase functional value to products. Essential fatty acids, aromas, antimicrobial agents, vitamins and antioxidants are examples of bioactive compounds widely used in food products. Flaxseed containing about 36–40% oil is the richest vegetal source of polyunsaturated fatty acids (PUFA) and can be considered as bioactive compound. The total PUFA amount of flaxseed oil is around 80–90%, and the high level of α-linolenic acid (ω-3) (40–60% of total fatty acids) characterizes this oil as one of the greatest sources of omega-3 (Goyal, Sharma, Upadhyay, Gill, & Sihag, 2014). Health benefits associated with flaxseed oil consumption have been demonstrated, which are related to prevention of cardiovascular diseases and cancer, reduction of cholesterol level, inflammations relief, protection against renal toxicity and autoimmune disorders (Rodriguez-Leyva, Bassett, McCullough, & Pierce, 2010; Wang et al., 2017). However, there are some challenges to incorporate PUFA rich oils into aqueous food matrices due to their lipophilic nature. In addition, the high oxidation rate of flaxseed oil shows the relevance to use encapsulating systems to protect this oil, which could be done in emulsions.

Simple and multiple emulsions present a high potential for encapsulation of active compounds, mainly because of the different polarity between disperse and continuous phases (McClements, 2010). Food emulsions are usually stabilized by monomeric surfactants, biopolymers and nano/micro nonsurfactant colloidal solids. These different substances can stabilize the interface of a colloidal system by different mechanisms (Sanfeld & Steinchen, 2008; Santana, Perrechil, & Cunha, 2013). Nano/microparticles are adsorbed onto the oil-water interface in Pickering emulsions, protecting emulsion droplets against flocculation, coalescence and Ostwald ripening by a steric barrier. In addition attraction forces between the particles at the interface and interactions between the particles and the liquid phases of the emulsion form an energy barrier (desorption energy) (Chevalier & Bolzinger, 2013; Costa, Gomes, & Cunha, 2018).

Cellulose is a linear biopolymer of β(1-4)-D-glucose residues linked by glycosidic oxygen bonds and it is the most abundant natural occurring polymer (Klemm, Heublein, Fink, & Bohn, 2005; Tang, Sisler, Grishkewich, & Tam, 2017). Different materials with technological

* Corresponding author.
E-mail address: rosiane@unicamp.br (R.L. Cunha).

https://doi.org/10.1016/j.foodres.2019.108746
Received 10 May 2019; Received in revised form 1 October 2019; Accepted 4 October 2019
Available online 31 October 2019
0963-9969/

applications can be obtained from cellulose such as microfibrillated cellulose, cellulose nanofibers, carboxymethyl cellulose, hydroxyethyl cellulose, microcrystalline cellulose and cellulose nanocrystals (Klemm et al., 2005). Cellulose nanoparticles are often prepared using a top-down approach, isolating the semi-crystalline individual nanofibers or extracting the crystalline portion in a controlled process (Capron, Rojas, & Bordes, 2017). The preparation of crystalline cellulose particles, such as colloidal microcrystalline cellulose or cellulose nanocrystals, usually employs strong acids or specific enzymes to hydrolyze the amorphous domain and release the crystalline domain (Domingues, Pereira, Sierakowski, Rojas, & Petri, 2016). Cellulose nanocrystals (CNCs) show a number of interesting properties such as low density, easy chemical manipulation, environmental sustainability, abundance of surface hydroxyl groups, high surface area (~250 m^2/g), high tensile strength (7500 MPa) and high stiffness (Young's modulus up to 140 GPa) (Grishkewich, Mohammed, Tang, & Tam, 2017; Lam, Male, Chong, Leung, & Luong, 2012). Different sources of cellulose, as well as different hydrolysis conditions, have considerable impact on the size distribution, crystalline structure and colloidal stability of the produced cellulose micro and nanoparticles (Capron et al., 2017; Oguzlu, Danumah, & Boluk, 2017).

Some works have shown the potential of cellulosic particles as emulsifiers and stabilizers mainly for oil-in-water emulsions. Microcrystalline cellulose deposited on oil-water interface can form a network around the oil droplets, providing a mechanical barrier that stabilizes the emulsion without decreasing the interfacial tension (Oza & Frank, 1986). Cellulose nanocrystals can also stabilize the oil/water interface promoting the formation of stable monodisperse oil droplets. The amphiphilic properties, size and shape of the particles, can influence the process of emulsification and stabilization (Kalashnikova, Bizot, Bertoncini, Cathala, & Capron, 2013; Kalashnikova, Bizot, Cathala, & Capron, 2011, 2012). However the emulsion stabilization mechanism produced by using anisotropic cellulose particles is not fully understood. Two parameters are currently recognized as crucial drivers of assembly and adsorption process of cellulose: the surface chemistry and particles shape (Capron et al., 2017).

Different mechanical processes can be used for emulsion production. Ultrasound is an emulsification process widely studied in the last years, which is based on the application of an acoustic field that results in cavitation phenomenon causing the formation of droplets (Jafari, Assadpoor, He, & Bhandari, 2008). Emulsification by high-intensity ultrasound can form stable emulsions with droplets in the submicrometer range and narrow size distribution (Abbas, Hayat, Karangwa, Bashari, & Zhang, 2013). A number of studies have been developed using ultrasound to form emulsions in order to be applied in encapsulation, solubilization, heteroagregation and controlled release of bioactive compounds (Furtado, Mantovani, Consoli, Hubinger, & da Cunha, 2017; Furtado, Michelon, de Oliveira, & da Cunha, 2016; Silva, Gomes, Hubinger, Cunha, & Meireles, 2015; Silva, Rosa, & Meireles, 2015; Silva, Zabot, Cazarin, Maróstica, & Meireles, 2016). Nevertheless there are few reports showing the effects of ultrasound process conditions on the emulsions stabilization by cellulose crystals (Paximada et al., 2016).

Therefore the aim of this research was to understand the mechanism of emulsion stabilization using cellulose crystals that are generally recognized as safe (GRAS) (Akhlaghi, Zaman, Peng, & Tam, 2015) for the food industry. For this purpose the effect of mechanical process conditions on the cellulose particles properties, the proportion of oil: cellulose particles on the emulsion properties, and the effect of the ultrasound process on the emulsions stabilized by cellulose particles were studied.

2. Material and methods

2.1. Material

Cellulose micro/nanocrystals (CMNC) were prepared from microcrystalline cellulose powder (20 μm) purchased from Sigma Aldrich Co. (St. Louis, EUA). Ultrapure water was provided from a Millipore Milli-Q system (resistivity 18.2 MU/cm), hydrochloric acid obtained from Synth (São Paulo, Brazil) and flaxseed oil was kindly donated by Cisbra (Rio Grande do Sul, Brazil).

2.2. Cellulose micro/nanocrystals (CMNC) preparation

Cellulose micro/nanocrystals (CMNC) were obtained from microcrystalline cellulose using hydrochloric acid (HCl) hydrolysis. For this, 28 g of microcrystalline cellulose was added to 1000 mL of 4 M hydrochloric acid under vigorous mechanical stirring at 80 °C during 3 h 45 min. After that, the dispersion was diluted two-fold in water and the suspension was rinsed with three repeated centrifugation cycles (10,000 rpm/15 min). Afterward, the dispersion was dialyzed using dialysis tubing cellulose membrane with 12–14 kDa molecular weight cut off purchased from Sigma Aldrich Co. (St. Louis, EUA), against deionized water until dispersion reached pH 6 (Araki, Wada, Kuga, & Okano, 1998).

2.3. Oil in water emulsion preparation

To understand the effect of emulsification process on the cellulose micro/nanocrystals, firstly an aqueous suspension of cellulose micro/nanocrystals (5% w/w) was submitted to the same conditions using only step of rotor-stator (Control UT), two steps of rotor-stator (UT + UT) and rotor-stator more ultrasound processes (UT + US) to produce emulsions. Oil-in-water (O/W) emulsions were prepared using different content of flaxseed oil (10%, 15% and 20% w/w) and cellulose micro/nanocrystals suspensions (2.5%, 3.75% and 5% w/w). Coarse emulsions were prepared by homogenizing cellulose micro/nanocrystals (CMNC) suspensions and flaxseed oil using a rotor-stator homogenizer Ultra Turrax model T18 (IKA, Staufen, Germany) for 3 min at 10,000 rpm. The oil phase was added dropwise to the CMNC suspension during coarse emulsion preparation. Fine emulsions were produced from the coarse emulsion (40 g) subjected to an ultrasound process in an ultrasonic processor (QR 750 W, Ultronique, Campinas, Brazil) with a 13 mm diameter titanium probe immersed 3 mm depth. Sonication time, power and frequency were fixed at 4 min, 525 W and 20 kHz, respectively (Furtado et al., 2016). A cold-water bath at 10 °C was connected to the ultrasonic processor to ensure that no significant heating occurred during the homogenization process. In order to evaluate the influence of the ultrasound on the emulsification process, the emulsion with flaxseed oil (10% w/w) and cellulose micro/nanocrystals (5% w/w) was prepared using only the rotor-stator homogenizer for 3 min at 10,000 rpm and 4 min at 13,000 rpm. This latter additional step was necessary to form stable emulsions (without ultrasound process).

2.4. Characterization of cellulose particles and emulsions

2.4.1. Particle size distribution

Droplets size distribution of the CMNC and emulsions was determined based on the static light scattering method using a Multi-Angle Static Light-Scattering Mastersizer (Mastersizer 2000, Malvern Instruments, Worcestershire, UK). Particle size distribution of CMNC was also determined using Dynamic Light Scattering (DLS) (more details of the methodology in the 2.4.2 section). Measurements were done in triplicate just after emulsions preparation and 7 days after storage. The surface area mean diameter ($D_{32} = \Sigma n_i d_i^3/\Sigma n_i d_i 2$ and the polydispersity (Span = $(D_{90}\text{-}D_{10})/D_{50}$)) were calculated. Where n_i is the number of particles with diameter d_i, and D_{10}, D_{50} and D_{90} are diameters at 10, 50 and 90% of cumulative volume, respectively.

2.4.2. Zeta potential and dynamic light scattering (DLS)

The zeta potential of CMNC suspended in Milli-Q water (0.01% w/

w) was determined in triplicate in a Nano-ZS Zetasizer equipment (Malvern Instruments, Worcestershire, UK).

DLS measurements were carried out after equilibrating CMNC suspensions (0.1% w/w) at 25 °C for 10 min. DLS measurements were conducted using the equipment working at 173° scattering angle. Mean particle size was reported as average hydrodynamic diameter ($D = KT/3\pi\eta D_t$), which was calculated according to the Stokes-Einstein relation for rod-shaped particles (Chang et al., 2016). Where K is Boltzmann's constant, T is the absolute temperature, η is the viscosity, and Dt is the translational diffusion coefficient. The polydispersity index (PDI) was calculated from cumulant analysis of the measured dynamic light scattering intensity autocorrelation function.

2.4.3. X-ray diffraction (XRD)

The aqueous CMNC suspension was freeze-dried (Terroni, model LS 3000, Brazil) for 24 h before the measurements. The degree of crystallinity was measured by X-ray diffraction (XRD) using a D8 Advance (Bruker Corporation, USA) operating at a voltage of 40 kV. The X-ray diffractograms were obtained at room temperature within a 2θ ranging from 5° to 40°. The crystallinity index of CMNC was calculated as the ratio of height between the maximum intensity of crystalline peak close to 2θ = 22° ($I_{22°}$) and the intensity of the non-crystalline material diffraction peak close to 2θ = 18° ($I_{18°}$) (Segal, Creely, Martin, & Conrad, 1959)

2.4.4. Fourier-transform infrared spectroscopy (FTIR)

Evaluation of functional groups was obtained with an infrared Fourier-transform spectrometer (Perkin Elmer, Spectrum One model, Ohio, USA) equipped with a universal attenuator total reflectance (UATR). The range of infrared region was 550–4000 cm^{-1} with a resolution of 4 cm^{-1} and 16 scans (Vicentini, Dupuy, Leitzelman, Cereda, & Sobral, 2005).

2.4.5. Interfacial tension and contact angle

The interfacial tension between the aqueous CMNC suspension and oil phase was measured before emulsion preparation by the pendant drop method using a Tracker S tensiometer (Teclis, Longessaigne, France). A syringe was used and assays were performed with the formation of a drop with 7 μL of the CMNC suspension (aqueous phase) in the oil phase. The contact angle between the oil phase and cellulose micro/nanocrystals was measured at 25 °C, using the same equipment with some adaptations. Assays were performed with the formation and detachment of an oil drop (4 μL) kept in contact with compressed samples of freeze-dried cellulose micro/nanocrystals. Contact angle values were automatically measured during 60 s.

2.4.6. Atomic force microscopy (AFM)

The aqueous CMNC suspension (1.0 μL) were placed on a grid with mica surface and dried at room temperature to perform AFM analysis. The images were obtained with a microscope (Anasys Instruments, model nano IR2-S, Santa Barbara, United States) equipped with a camera, under controlled conditions (relative moisture = 10% and temperature = 25 °C).

2.4.7. Kinetic stability –Laser scanning turbidimetry

Emulsion stability was measured using the optical scanning instrument Turbiscan ASG (Formulaction, Toulouse, France). Emulsions were placed in cylindrical glass tubes with screw cap (14 cm height; 1.6 cm diameter) and stored at 25 °C. The backscattered signal of fresh emulsion (just after preparation) and stored during 28 days was scanned from the bottom to the top with a source light at 880 nm.

2.4.8. Optical and confocal laser scanning microscopy

Optical microscopy was performed on a Carl Zeiss Axio Scope A1 microscope (Zeiss, Oberkochen, Germany) and the images were captured with the software AxioVision Rel. 4.8 (Carl Zeiss, Germany). Confocal laser scanning microscopy was performed on a Zeiss LSM780-NLO confocal on an Axio Observer Z.1 microscope (Carl Zeiss AG, Germany) using 63x and 100x objectives. Cellulose crystals-stabilized emulsions were mixed to Congo Red, stirred for 5 min, to dye the cellulose particles. Images were performed using 488 nm laser line for excitation and 605 nm emission filters for Congo Red.

2.4.9. Rheological assays

Flow curves of emulsions were obtained using a stress-controlled rheometer (AR1500ex, TA Instruments, England) with a cone-plate geometry (diameter = 40 mm, truncation 53 μm). The analysis was done within the shear rate range between 0 and 300 s^1, in a three-steps sequence: up-down-up. The third curve data was fitted to the Herschel Buckley model ($\sigma = \sigma_o + k(\dot{\gamma})^n$). σ is the shear stress (Pa), σ_0 is the yield stress (Pa), $\dot{\gamma}$ is the shear rate (s^{-1}), k is the consistency index (Pa s^n) and n is the flow behavior index (dimensionless). The emulsions were evaluated just after their preparation and 7 days after storage. The measurements were made in duplicate at 25 °C.

2.4.10. Statistical analysis

Results from droplets size distribution, rheological assays, zeta potential, dynamic light scattering and contact angle were evaluated by analysis of variance (ANOVA) using 5% level of significance. The differences between the treatments were evaluated by the Tukey procedure ($p < 0.05$). Triplicate measurements were performed. The statistical analyses were carried out using the software STATISTICA 7.0 (Statsoft Inc., Tulsa, USA).

3. Results

3.1. Effect of the emulsification process on the cellulose particles

Table 1 shows the cellulose micro/nanocrystals properties dispersed in water after the different mechanical processes using the same conditions to produce emulsions. Hydrolysis process reduced the microcrystalline cellulose size around four times, since the mean diameter of

Table 1
Properties of cellulose micro/nanocrystals (CMNC) dispersed in water and subjected to different mechanical processes.

Sample	Particle size distribution				Crystallinity (ICr %)	Zeta potential (mV)
	Mastersizer – Static light scattering measurement		Zetasizer – Dynamic Light Scattering measurement			
	1st peak (D_{32}/μm) (% Volume)	Span	2nd peak (nm) (% Intensity)	PDI		
MCC (Sigma Aldrich)	20.31 ± 0.32 ^{a}	3.83 ± 0.57^{a}	–	–	81.38 ± 0.27^{c}	−10.75 ± 0.65^{a}
Control UT	5.87 ± 0.02^{b}	7.24 ± 0.57^{c}	326.4 ± 43.4^{a}	0.31 ± 0.02^{a}	74.66 ± 0.63^{a}	−25.14 ± 0.15^{b}
UT + UT	5.58 ± < 0.01^{c}	3.92 ± 0.18^{a}	315.4 ± 65.1^{a}	0.67 ± < 0.01^{b}	77.95 ± 0.39^{b}	−27.76 ± 0.40^{bc}
UT + US	5.66 ± < 0.01^{d}	5.48 ± 0.69^{b}	274.9 ± 58.4^{b}	0.43 ± 0.04^{c}	79.10 ± 0.81^{b}	−30.83 ± 0.87^{bc}

Control UT: (3 min/10,000 rpm); UT + UT: (3 min/10,000 rpm + 4 min/13,000 rpm); UT + US: (3 min/10,000 rpm + 4 min/525 W). Different letters in the same column indicate significant difference ($p < 0.05$). UT = rotor-stator process, US = ultrasound process.

the microcrystalline cellulose was around 20 μm. Hydrogen ions produced by acid ionization could break the cellulose glycosidic bonds reducing the particle size and resulting in a loss of non-crystalline region (Bondeson, Mathew, & Oksman, 2006). However the presence of bimodal size distribution indicated that the process was not enough efficient to produce only nanoparticles. Mechanical processes using rotor-stator and ultrasound only promoted a slight reduction of the cellulose crystals size, showing that these processes could break the structure of cellulose crystals, but maintained the bimodal distribution with part of the particles within the microscale. This finding is interesting for Pickering emulsions, since micrometric and nanometric cellulose particles act in different ways to form and stabilize emulsions (Oza & Frank, 1986). A deeper discussion about these mechanisms is presented in the 3.2 section.

FTIR spectroscopy technique was used to evaluate the main functional groups of microcrystalline (MCC) and cellulose micro and nanocrystals (CMNC). This analysis aimed to observe if the mechanical processes could change the chemical structure of the cellulose crystals. Fig.S1 in supplementary file shows the FTIR-UATR spectra of the samples. The peak at 3320–3330 cm^{-1} corresponds to alcoholic hydroxyl groups. The amount of hydroxyl groups can increase in cellulose crystals after acid treatment (Hedjazi & Razavi, 2018). However changes in the amount of hydroxyl groups were not observed. Less intense peaks between 2890 cm^{-1} and 2350 cm^{-1} correspond to C-H bonds, while the peak observed at 1410–1430 cm^{-1} is associated to H-C-H and O-C-H stretching. Peaks at 1150–1160 cm^{-1} indicate the presence of cellulose crystals and between 900 cm^{-1} and 1100 cm^{-1} show that cellulose structures were primarily cellulose I. Changes in the spectra of cellulose structures were not observed using different mechanical processes conditions.

The kinetics of interfacial tension between flaxseed oil and the CMNC aqueous suspensions was investigated during 33 min (Fig. 1). The interfacial tension between flaxseed oil and water was also measured to evaluate the surface activity of CMNCs. The initial interfacial tension between flaxseed oil and aqueous suspensions containing either cellulose micro/nanocrystal (CMNC UT), or cellulose micro/nanocrystal treated with rotor-stator (CMNC UT + UT), or cellulose micro/nanocrystal treated with rotor-stator and ultrasound (CMNC UT + US) was around 20–22 mN/m. All the samples reached the equilibrium interfacial tension ranging from 8.5 to 9 mN/m after approximately 20 min. Kinetics of the aqueous phase containing CMNC suspensions

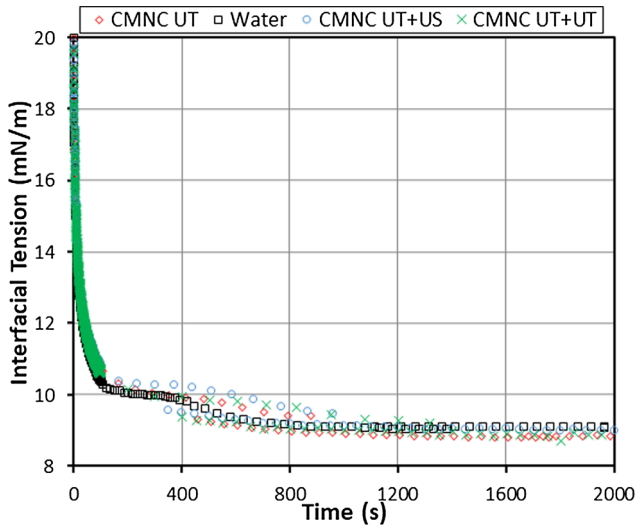

Fig. 1. Dynamic interfacial tension between flaxseed oil and water or cellulose micro/nanocrystals (CMNC) aqueous suspensions obtained after different homogenization conditions using rotor-stator (CMNC UT + UT), ultrasonic (CMNC UT + US) and control: UT.

was similar to the water, indicating that CMNC did not change the interfacial tension between the aqueous suspensions and flaxseed oil. Water-in-soybean oil Pickering emulsions containing alkyl intercalated cellulose nanocrystals were stabilized by steric hindrance rather than a mechanism of interfacial tension reduction, because the interfacial tension at the soybean oil-water interface was not reduced in the presence of alkyl intercalated CNCs (Guo, Du, Gao, Cao, & Yin, 2017). In addition the equilibrium interfacial tension between water and flaxseed oil was lower than other oils (Gomes, Costa, & Cunha, 2018; Gomes, Costa, de Assis Perrechil, & da Cunha, 2016). Flaxseed oil could spontaneously form nanoemulsion even without any surfactant, because flaxseed oil showed the lowest interfacial tension with water (4 mN/m) in comparison with soybean and jojoba bean oil (Adamczak, Para, Simon, & Warszyński, 2013).

Contact angle measurement is widely used to evaluate the wettability of films with hydrophilic or hydrophobic materials (Yuan & Lee, 2013). The effect of mechanical processes on the hydrophobicity of CMNC was measured by the contact angle of flaxseed oil and water in CMNC films (Fig.S2 in supplementary file). Within a time range < 2 s of analysis, the contact angle between the water and a microcrystalline cellulose film varied between 27° and 13° (Pang, Liu, Liu, Peng, & Zhang, 2018), which was also observed in our results. When the oil and water drop spreads further on the cellulose micro/nanocrystal film, the contact angle was low and a great affinity between the phases was observed between oil and water with cellulose crystals. This behavior could be due to the low interfacial tension between flaxseed oil and water (< 10 mN/m), so the cellulose particles will have an affinity for both water and flaxseed oil (Fig. 1). The contact angle values were very small in the presence of both phases, showing values between 16° and 20° with flaxseed oil and between 12° and 15° with water. This suggests that the cellulose crystals can form oil-in-water or water-in-oil emulsions, but the prevailing amount of water (80–90% w/w) favored the formation of oil-in-water emulsions (Hunter, Pugh, Franks, & Jameson, 2008). Shear and cavitation effects produced by rotor-stator homogenizer and ultrasound only showed a slight effect on the contact angle values.

Fig.S3 in supplementary file shows the X-ray diffraction pattern obtained for cellulose micro/nanocrystals. Patterns of CMNC UT, CMNC UT + UT and CMNC UT + US showed two peaks, closed to 2θ = 18°and 2θ = 22°. X-ray diffraction pattern of the three treatments displays a major presence of cellulose I. Crystallinity is an important factor determining thermal and mechanical properties of cellulose (Tang, Yang, Zhang, & Zhang, 2014). Crystallinity index of the CMNCs is presented in Table 1, showing that mechanical processes promoted a slight decrease in CMNCs crystallinity when compared with MCCs. This indicates that the intermolecular hydrogen bonds of cellulose crystals may broke during the homogenization process, causing the collapse of the crystalline structure (Costa, Gomes, Tibolla, Menegalli, & Cunha, 2018; Winuprasith & Suphantharika, 2013). Crystallinity index values were similar to those obtained by other authors. For example Li et al. (2012) observed that crystallinity index of cellulose nanocrystals was around 73% after ultrasonic treatment (1500 W/15 min). However non-selective effect of ultrasonication can remove both amorphous and crystalline domains of cellulose. Therefore, low-ultrasonic treatment could be more favorable on the micro/nanocrystals crystallinity than high-ultrasonic treatment.

Electrostatic stability of cellulose crystals was determined by the zeta potential (Table 1). Cellulose crystals showed good stability against agglomeration due to electrostatic repulsion, since stable suspension of cellulose crystals should have an zeta potential values lesser than −30 mV or greater than 25–30 mV (Mohaiyiddin et al., 2016; Naduparambath et al., 2018). The high mechanical energy supplied by ultrasound could promote better dispersion of the suspension and greater contact between CMNCs and oxygen, favoring the generation of negative charge on the particles surfaces due to the partial oxidation and reduction of particles size (Costa et al., 2018; Winuprasith &

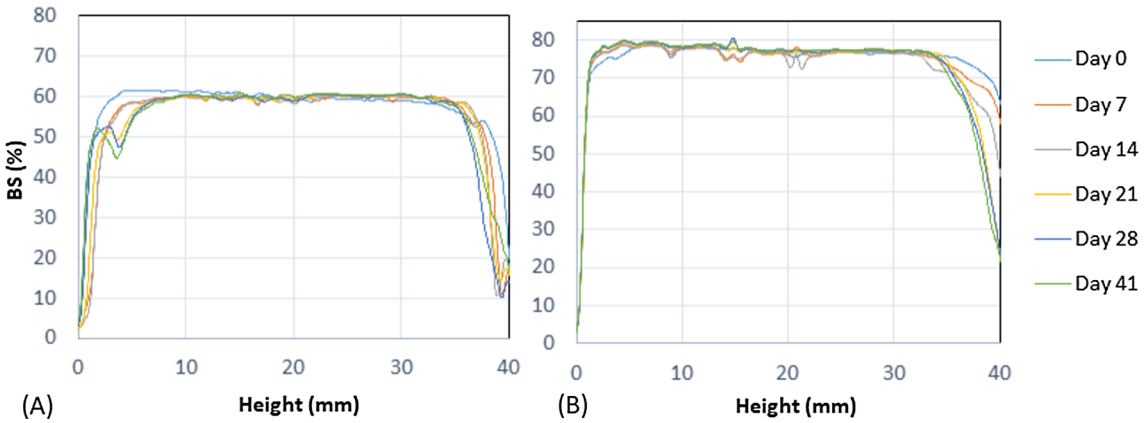

Fig. 2. Backscattering profiles (0, 7, 14, 21, 28 and 41 days of storage) of emulsions stabilized with cellulose micro/nanocrystals (CMNC) (5% w/w) obtained from different homogenization conditions using rotor-stator (UT + UT) (A) and rotor-stator and ultrasound process (UT + US) (B).

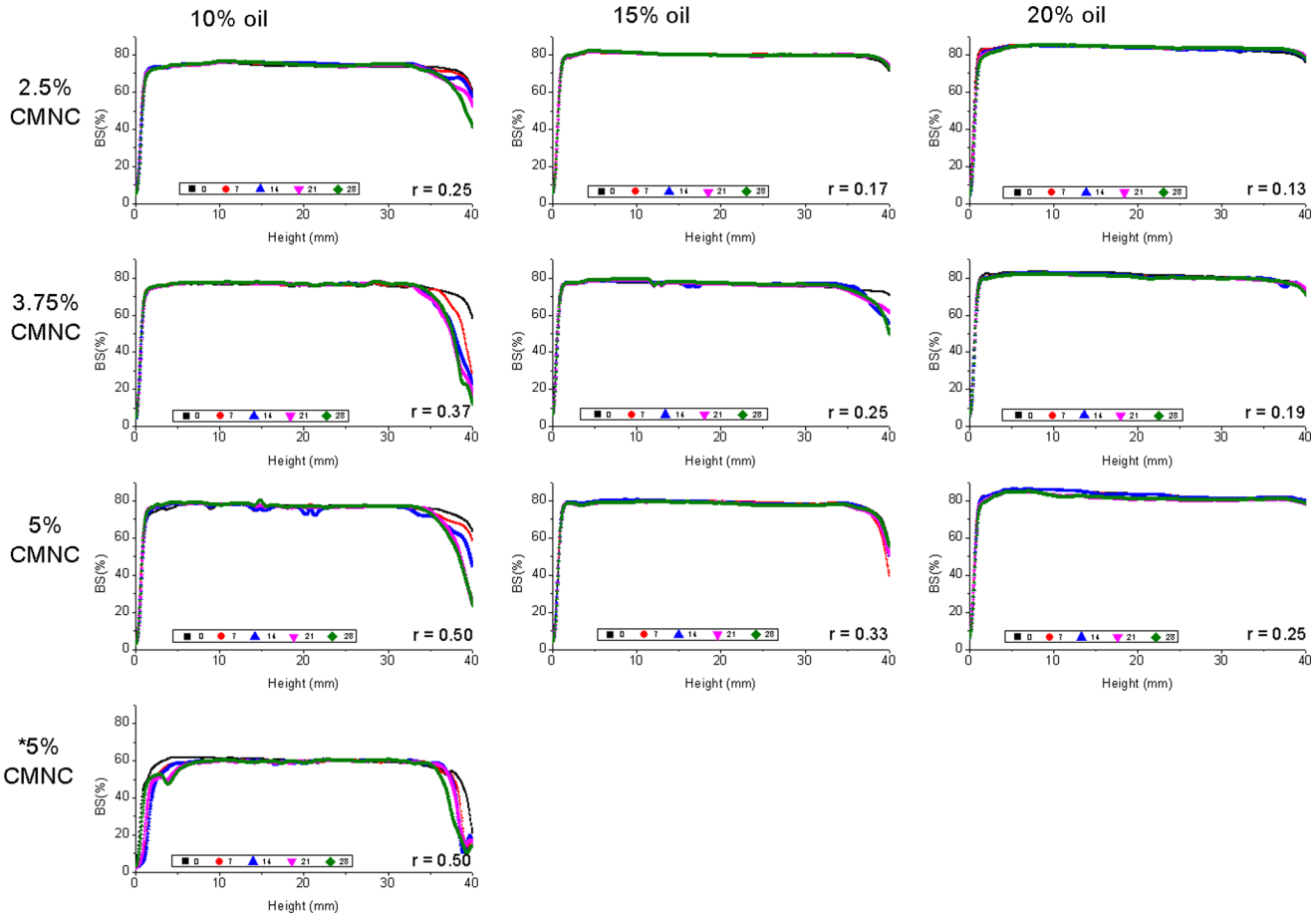

Fig. 3. Backscattering profiles (0, 7, 14, 21, and 28 days of storage) of emulsions stabilized with different proportions of cellulose micro/nanocrystals (CMNC) and flaxseed oil homogenized with rotor-stator and ultrasound process (UT + US). r = ratio between CMNC concentration and oil concentration. Condition with * is an emulsion produced only with rotor stator process (UT + UT).

Suphantharika, 2013).

Fig.S4 in supplementary file shows the atomic force microscopy (AFM) obtained for cellulose untreated microcrystalline and cellulose micro/nanocrystals (CMNC). Our results show that microcrystalline cellulose, before all treatments, shows an agglomerate with large size, as expected (20 μm). After the acid treatment, centrifugation, dialysis and agitation with rotor-stator (UT) and ultrasound process (US), CMNCs were dispersed in a more separated network, with the shape of needles that is characteristic of cellulose crystals (Hedjazi & Razavi, 2018).

3.2. Different proportions of cellulose crystals and flaxseed oil change the properties of the emulsions

Kinetic stability of the emulsions was determined after 0 (fresh emulsion), 7, 14, 21 and 28 days of storage at 25 °C. Kinetic stability of the emulsions stabilized with cellulose micro/nanocrystals (CMNC) (5% w/w) obtained from different homogenization conditions using rotor-stator (UT + UT) and rotor-stator and ultrasound process (UT + US) was performed up to 28 days of storage at 25 °C. The optical analyzer (Turbiscan) apparatus has been successfully used to study the stability

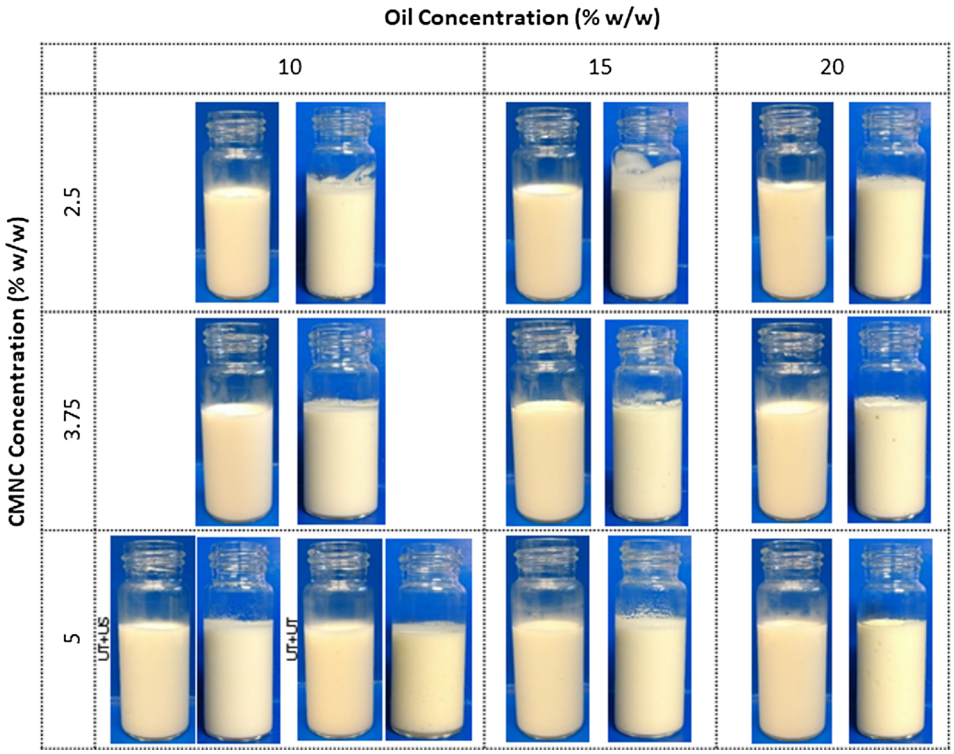

Fig. 4. Visual aspect of fresh emulsions (left) and after 7 days of storage (right), stabilized with different proportions of cellulose micro/nanocrystals (CMNC) related to flaxseed oil.

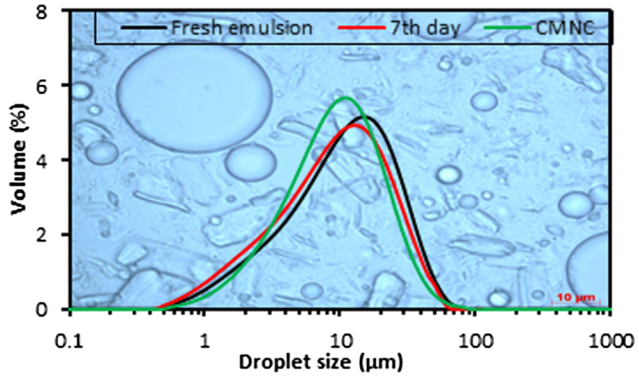

Fig. 5. Micrographs and particle size distribution of emulsions stabilized with different proportions of cellulose micro/nanocrystals (CMNC) related to flaxseed oil. CMNCs were obtained from homogenization condition using rotor-stator (UT + UT). Scale bar: 10 µm.

of emulsions, foams and concentrated colloidal dispersions (Lemarchand, Couvreur, Vauthier, Costantini, & Gref, 2003; McClements, 2007; Mengual, Meunier, Cayre, Puech, & Snabre, 1999). Turbiscan allows observing destabilization phenomena (coalescence, flocculation, creaming or sedimentation) much earlier than the operator naked eye, especially for opaque and/or concentrated systems (Lemarchand et al., 2003). The backscattering (BS) profiles versus the height of the glass tube are presented in Figs. 2 and 3. High BS percentages indicate great concentration and/or opacity of the samples. Fresh emulsion produced using rotor-stator (control) presented BS values around 60%, while the emulsion produced by an additional rotor-stator and ultrasound processing presented values about 70 and 80%, respectively. BS values are inversely proportional to the droplet size, which means that the ultrasound process further increased the dispersion of cellulose micro/nanocrystals and oil into the water phase, or increased the drops concentration by reducing the droplet size.

The BS of emulsion produced using only rotor-stator (UT + UT) decreased at the top (30–40 mm) of glass tube (Fig. 2) along the days. These profiles indicate destabilization process due to the creaming of oil droplets at the top of glass tube or sedimentation of possible CMNC excess, promoting an emulsion clarification (clarified serum on the bottom and cream layer on the top).

Fig. 3 shows the BS profiles of emulsions produced by ultrasonic process varying the oil and CMNC concentration. Emulsions containing 10% (w/w) oil showed that the amount of cellulose crystals was not enough or was in excess to prevent the system destabilization. BS decreased at the top of the emulsions, which is associated to an increase of the oil concentration (creaming), and/or the sedimentation based on the excess of CMNC (serum layer). However BS on the top (30–40 mm) increased as the oil content increased, allowing to infer that even 2.5% (w/w) of CMNC was used in excess (with 10% oil), i.e., the CMNC covered all the oil droplets and the excess was dispersed into the aqueous phase of the system. Consequently, the destabilization mechanism was driven by sedimentation of CMNC (at least partly) producing a clarified layer at the top of the sample. During the preparation of oil-in-water emulsions, bridging flocculation is possible if the amount of emulsifier or stabilizing particles available during homogenization is not enough to fully recover the newly created interface (Dickinson & Galazka, 1991; Dickinson, Flint, & Hunt, 1989). Bridging may occur in the presence of biopolymers particles in excess (polysaccharide and protein molecules) since the forces between them are strongly attractive, allowing the linkage of droplets by the CMNCs adsorbed onto the surface of two or more droplets (Dickinson, 1998).

The BS profiles of emulsions with the ratio (CMNC concentration/oil concentration) 0.17, 0.25 and 0.33 with 15% w/w oil supports this argumentation since the same behavior was observed although with less intensity than 10% oil. At the ratio (CMNC concentration/oil concentration) 0.13, 0.19 and 0.25 with 20% w/w oil, such a behavior was not observed, which means that a good proportion between CMNC and oil could be achieved and/or the higher number of droplets (and consequent interaction between them) avoided CMNC sedimentation.

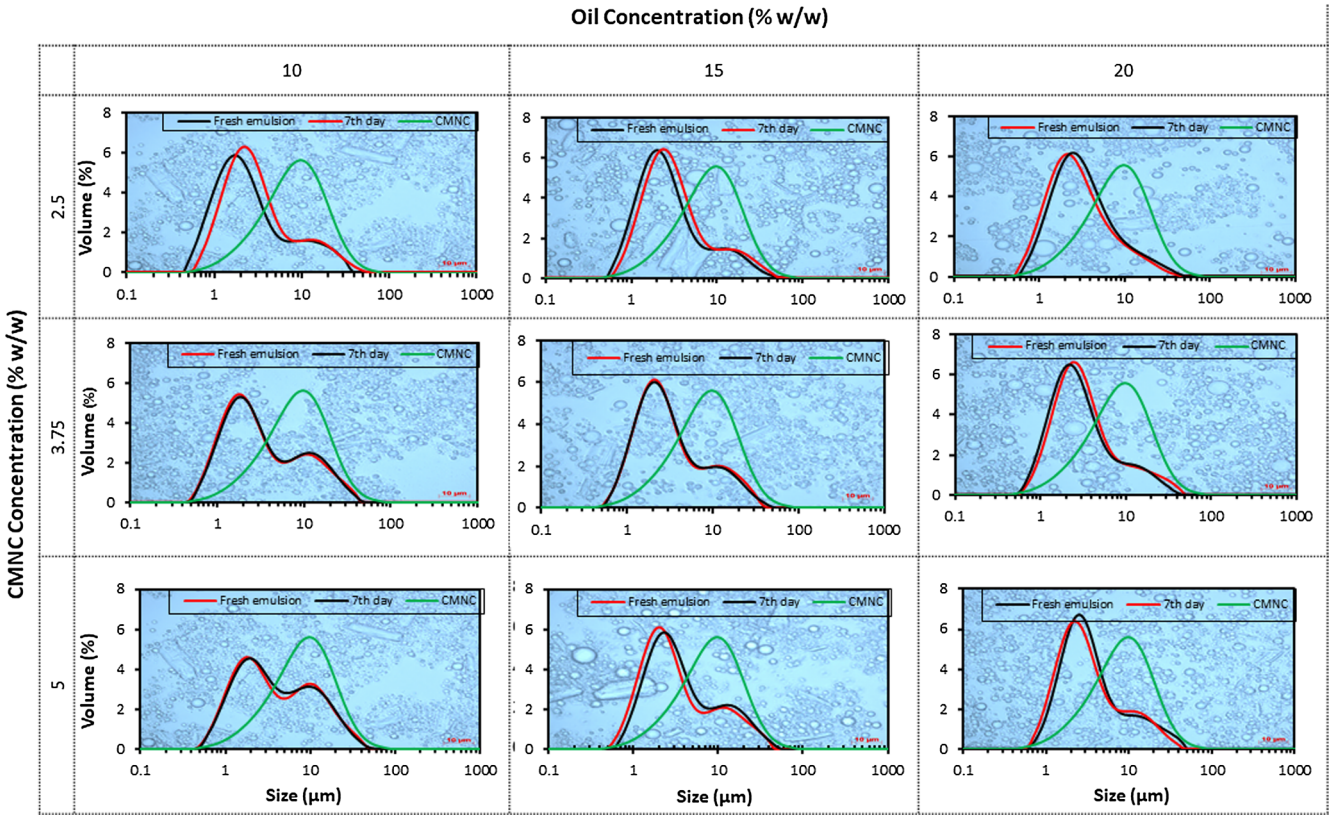

Fig. 6. Micrographs and particle size distribution of emulsions stabilized with different proportions of cellulose micro/nanocrystals (CMNC) related to flaxseed oil. CMNCs obtained from homogenization condition using rotor-stator and ultrasound process (UT + US). Scale bar: 10 µm.

Interestingly, at this oil concentration, the BS slightly increased with the CMNC content increase, which probably occurred due to the increase of viscosity making difficult the CMNC sedimentation. The oil concentration is an important factor for the stability of the emulsions as can be observed for emulsions with the same ratio r = 0.25, since the emulsion with 20% oil was more stable during the storage time. In addition, it is noteworthy that the sedimentation phenomenon was not observed on the BS profiles below 30 mm, which could be attributed to the high particles concentration overcoming the equipment limit detection. The visual aspect of these emulsions is presented in Fig. 4, immediately after preparation and after 7 days of storage at room temperature. All the emulsions were opaque, homogeneous and showed only one phase, even after 7 days of storage.

The droplet size (D_{32}) was determined for fresh emulsion and at the 7th day of storage. An increase in the droplets size is associated to the coalescence favoring emulsion destabilization (McClements, 2005). Fresh emulsion produced using rotor-stator presented a monomodal size distribution, but the highest values of droplet size (mode around 15 µm) (Fig. 5). The size distribution of the cellulose particles in Fig. 5 is representing the values presented in the third line of Table 1 (UT + UT). In this condition of emulsions preparation, the droplet size distribution and the CMNC size distribution were similar. In this case, the cellulose particles probably may form a three- dimensional network in the continuous phase, which immobilize the oil droplets and enhances emulsion physical stability (Horozov & Binks, 2006). Fresh emulsion produced using the rotor-stator followed by ultrasound process showed a bimodal size distribution, but with smaller droplet size values (Fig. 6). Comparing both processes rotor-stator (UT + UT) and ultrasound (UT + US), the UT + US process reduced the droplet size in 44% using the same emulsion condition (5% (w/w) of CMNC and 10% (w/w) of flaxseed oil). The size distribution of the cellulose particles in Fig. 6 is representing the mean value presented in the fourth line of Table 1 (UT + US). Cavitation forces are predominant in ultrasound process generating unstable bubbles and yielding implosions. These implosions (disruption and mixing) cause the rupture of droplets and may also disrupt cellulose crystals, contributing to the formation of micrometer-sized emulsion droplets. At the same time, regions of hydrodynamic shear are created close to the tip of the probe, where emulsification takes place (Costa, Gomes, Andrade, & Cunha, 2017; McClements, 2007; Silva, Zabot, Toledo Hijo, & Meireles, 2017).

Table 2 shows mean the droplet size (D_{32}) and polydispersity index (Span) of the emulsions. Droplet size increased when the CMNC concentration was increased keeping fixed the oil concentration, indicating that there is an adequate proportion between CMNC and oil, as mentioned before. Increase of droplet size associated to increase of CMNC concentration could affect the continuous phase viscosity (Chevalier & Bolzinger, 2013; Li et al., 2018). Increasing CMNC content also increased the total solid content of the dispersed phase, and consequently led to a higher viscosity of the emulsion. However, the droplet size also slightly increased when the concentration of oil was increased and a same concentration of cellulose crystal was kept fixed, which was confirmed by the emulsions structure (Fig. 6). A higher oil content results in a greater proximity of the droplets, which could favor the coalescence or agglomeration of droplets (McClements, 2005). However no significant differences in droplet size were observed after 7 days of storage for most of emulsions, showing that they present a good stability. A trend was observed in the polydispersity, since it decreased as the amount of oil increased in the emulsion. A higher number of cellulose particles dispersed in continuous phase could move towards the oil droplets increasing oil content, recovering interface and increasing mean droplets size (Table 2). Therefore, the decreased number of cellulose particles in the continuous phase contributed to the lower polydispersity (Dapčević Hadnađev, Dokić, Krstonošić, & Hadnađev, 2013).

Confocal micrographs showed the cellulose crystals (red color) distribution onto the emulsion droplets (Fig. 7). Immediately after

Table 2
Mean droplets size of emulsions produced from different mechanical processes and ratio between CMNC and oil concentration.

Process	CMNC (% w/w)	10% oil (w/w)				15% oil (w/w)				20% oil (w/w)			
		0 day		7th day		0 day		7th day		0 day		7th day	
		D_{32} (μm)	Span	D_{32} (μm)	Span	D_{32} (μm)	Span	D_{32} (μm)	Span	D_{32} (μm)	Span	D_{32} (μm)	Span
UT + US	2.5	1.96 ± 0.07^{Aa}	$5.49 \pm 0.43^{(Ad)}$	2.16 ± 0.04^{Ab}	$4.71 \pm 0.34^{(Ae)}$	2.21 ± 0.02^{Ab}	$4.73 \pm 0.10^{(Ae)}$	2.29 ± 0.02^{Abc}	$4.32 \pm 0.16^{(Af)}$	2.28 ± 0.04^{Abc}	$3.26 \pm 0.17^{(Ag)}$	2.31 ± 0.02^{Ac}	$3.19 \pm 0.15^{(Ag)}$
	3.75	2.29 ± 0.06^{Ba}	$5.77 \pm 0.19^{(Ac)}$	2.37 ± 0.05^{Bb}	$5.56 \pm 0.13^{(Bc)}$	2.43 ± 0.03^{Bb}	$4.98 \pm 0.18^{(Ad)}$	2.43 ± 0.03^{Bb}	$4.78 \pm 0.18^{(Bd)}$	2.38 ± 0.05^{Ab}	$3.99 \pm 0.15^{(Be)}$	2.39 ± 0.03^{Ab}	$3.92 \pm 0.11^{(Be)}$
	5	2.59 ± 0.04^{Ca}	$4.68 \pm 0.38^{(Ba)}$	2.66 ± 0.05^{Ca}	$4.49 \pm 0.22^{(Aa)}$	2.42 ± 0.07^{Bb}	$5.41 \pm 0.19^{(Bb)}$	2.49 ± 0.03^{Bb}	$5.07 \pm 0.28^{(Bc)}$	2.52 ± 0.07^{Bc}	$4.36 \pm 0.35^{(Cd)}$	2.55 ± 0.01^{Bc}	$4.38 \pm 0.12^{(Cd)}$
UT + UT	5	5.41 ± 0.21^{Da}	$2.46 \pm 0.04^{(Db)}$	5.36 ± 0.03^{Da}	$2.58 \pm 0.03^{(Cb)}$	–	–	–	–	–	–	–	–

Different letters indicate significant difference ($p < 0.05$) for the same property. Small letters: differences in the same line between the storage time. Capital letters: differences in the same column between CMNC concentration. For Span statistical analysis: letters are presented inside parenthesis.

emulsion preparation, the largest microcrystals are between the oil droplets, preventing the creaming. The flaxseed oil droplets were completely surrounded by cellulose particles, which could be partly a consequence of Pickering-type stabilization since the cellulose particles may also form a three dimensional network in the continuous phase, increasing the emulsion stability. This suggests that the particle adsorption could be by depletion attraction (Hu, Ballinger, Pelton, & Cranston, 2015; Kalashnikova, Bizot, Cathala, & Capron, 2011; Schröder, Sprakel, Schroën, Spaen, & Berton-Carabin, 2018). Confocal micrographs confirm the results of droplets size, since emulsions formed from ultrasound process showed smaller droplet size compared to the emulsion produced with rotor-stator.

Rheological properties of emulsions fitted very well to Herschel – Bulkley model, showing pseudoplasticity and yield stress. Apparent viscosity of emulsions with different concentration of cellulose particles and oil are presented in Table 3. Increasing CMNC content increased the emulsion apparent viscosity, once rigid particles disturb the normal flow of the fluid causing greater energy dissipation due to friction (McClements, 2005). Therefore the continuous phase may be "indirectly" stabilizing the droplets by entrapment. Cellulose crystals influence emulsion stability by apparently affecting both the interfacial region and the continuous phase (Capron et al., 2017; Kalashnikova et al., 2013). In addition, the apparent viscosity and shear stress of the systems increased as the oil content increased because a higher number of droplets increases the energy dissipation associated with fluid flow (McClements, 2005). For fresh emulsion, the ultrasonic process increased the apparent viscosity around 20% in comparison to the rotor-stator process. After seven days of storage, for all the conditions the viscosity increased when compared with the fresh emulsion. This behavior was more evident with 10 and 15% oil, which could be associated to more perceptible cremeation effects in these emulsions. Therefore a more concentrated portion of the emulsions with 10 and 15% of oil (cream phase) could be taken out to be analyzed in the rheometer. A viscoelastic network may be formed during the storage probably due to the high quantity of cellulose crystals dispersed in the continuous phase. Cellulose crystals are not only a viscosity builder in water-oil systems, but they are wetted by oil as well as water. For this, it would be also expected cellulose particles adsorption onto oil-water interface, thereby providing a mechanical barrier to emulsion droplet coalescence (Li et al., 2018; Oza & Frank, 1986).

4. Conclusions

The effect of mechanical process conditions on the cellulose particles properties, the proportion oil:cellulose particles on the emulsion properties, and the effect of the ultrasound process on the emulsions stabilized by particles were studied. Mechanical processes using rotor-stator followed by ultrasound promoted a reduction on the cellulose crystals size, showing that these processes can break the structure of cellulose crystals. However after the hydrolysis and mechanical processes the cellulose crystals showed bimodal particle size distribution showing some advantages to emulsion stabilization. The mechanical processes promoted small changes in the CMNC properties during the emulsion formation. Our results allowed establishing some mechanisms to explain the phenomena associated to stabilization of o/w emulsions containing CMNC particles. After emulsion preparation, flaxseed oil droplets were surrounded by smaller crystals but the interfacial reduction mechanism was not relevant, corroborating that the CMNC particles can initially stabilize oil-in-water interfaces by the Pickering mechanism. The effect of the proportion between the concentration of cellulose particles and oil was relevant for stabilizing properties. An excessive amount of cellulose particles was associated to the bridging flocculation phenomenon, in which the forces between particles are strongly attractive promoting the creaming. Therefore an ideal proportion of CMNC and oil should be achieved to produce more stable emulsions. The viscosity increasing during storage suggests that the

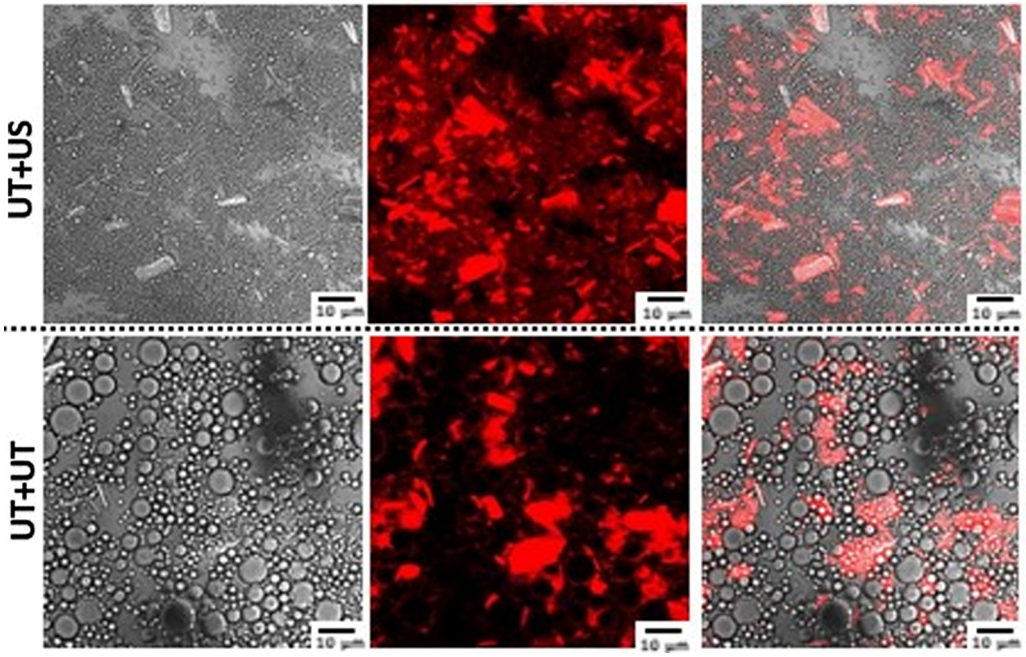

Fig. 7. Optical and Confocal micrograph of emulsion stabilized with cellulose micro/nanocrystals (CMNC) (5% w/w) obtained with rotor-stator and ultrasound process (UT + US) and rotor-stator (UT + UT). Scale bar: 10 μm.

Table 3
Apparent viscosity at 10 s^{-1} of emulsions produced by different process and ratio between CMNC and oil concentration.

Process	CMNC (%, w/w)	10% oil (w/w)		15% oil (w/w)		20% oil (w/w)	
		η 10 s^{-1} (mPa.s)		η 10 s^{-1}(mPa.s)		η 10 s^{-1} (mPa.s)	
		0 day	7th day	0 day	7th day	0 day	7th day
UT + US	2.5	108.88 ± 0.57^{aA}	120.37 ± 0.29^{bA}	160.22 ± 0.47^{cA}	176.79 ± 0.52^{fA}	169.14 ± 1.32^{dA}	172.79 ± 0.43^{eA}
	3.75	218.08 ± 0.12^{aB}	230.28 ± 0.32^{bC}	327.94 ± 0.68^{eB}	403.89 ± 0.88^{fB}	254.01 ± 0.17^{cB}	268.90 ± 0.76^{dB}
	5	336.89 ± 0.43^{aD}	405.95 ± 0.69^{dD}	469.64 ± 0.24^{eC}	542.38 ± 0.36^{fC}	344.46 ± 0.48^{bC}	353.68 ± 0.62^{cC}
UT + UT	5	264.71 ± 0.73^{aC}	207.62 ± 0.43^{bB}	–	–	–	–

Different letters indicate significant difference ($p < 0.05$). Small letters: differences in the same line. Capital letters: differences in the same column.

high amount of big cellulose crystals contribute to form a viscoelastic network. It was clear that the ultrasound process helped to improve emulsions stability that showed higher kinetic stability, lower droplet size and higher emulsion viscosity. We hope the results presented here may contribute to better understanding of the stabilizing mechanisms of emulsions containing cellulose crystals. Crystals with different sizes can contribute effectively to stabilize emulsion in two ways: nanoparticles established formation of Pickering emulsion while microparticles formed a viscoelastic network entrapping oil droplets. This could be an attractive system for encapsulation of lipophilic compounds such as vitamins, aroma compounds, fatty acids to be applied in various domains including food, cosmetics, and pharmaceutical applications.

Declaration of Competing Interest

The authors declared that there is no conflict of interest.

Acknowledgments

The authors thank Coordenação de Aperfeiçoamento de Pessoal de Nível Superior (CAPES -DEA/FEA/PROEX) and Fundação de Apoio à Pesquisa do Estado de São Paulo (FAPESP) for financial support (Process numbers 2007/58017-5 and 2011/06083-0). Aureliano Agostinho Dias Meirelles thanks CAPES – Brazil for the PhD fellowship. Ana Letícia Rodrigues Costa Lelis thanks CNPq – Brazil (CNPq 140710/2015-9). Rosiane Lopes Cunha thanks CNPq – Brazil (CNPq 307168/2016-6) for the productivity grant. The authors thank the Laboratory for Surface Science (LCS) of the National Nanotechnology Laboratory (LNNano) (Campinas, Brazil) for AFM analyses.

Appendix A. Supplementary material

Supplementary data to this article can be found online at https://doi.org/10.1016/j.foodres.2019.108746.

References

Abbas, S., Hayat, K., Karangwa, E., Bashari, M., & Zhang, X. (2013). An overview of ultrasound-assisted food-grade nanoemulsions. *Food Engineering Reviews, 5*(3), 139–157.

Adamczak, M., Para, G., Simon, C., & Warszyński, P. (2013). Natural oil nanoemulsions as cores for layer-by-layer encapsulation. *Journal of Microencapsulation, 30*(5), 479–489.

Akhlaghi, S. P., Zaman, M., Peng, B., & Tam, K. C. (2015). CHAPTER 8 – Cationic Cellulose and Chitin Nanocrystals for Novel Therapeutic Applications. In Cationic Polymers in Regenerative Medicine (pp. 197–227). The Royal Society of Chemistry.

Araki, J., Wada, M., Kuga, S., & Okano, T. (1998). Flow properties of microcrystalline cellulose suspension prepared by acid treatment of native cellulose. *Colloids and Surfaces A: Physicochemical and Engineering Aspects, 142*(1), 75–82.

Bondeson, D., Mathew, A., & Oksman, K. (2006). Optimization of the isolation of nanocrystals from microcrystalline celluloseby acid hydrolysis. *Cellulose, 13*(2), 171.

Capron, I., Rojas, O. J., & Bordes, R. (2017). Behavior of nanocelluloses at interfaces. *Current Opinion in Colloid & Interface Science, 29*, 83–95. https://doi.org/10.1016/j.cocis.2017.04.001.

Chang, H., Luo, J., Bakhtiary Davijani, A. A., Chien, A.-T., Wang, P.-H., Liu, H. C., & Kumar, S. (2016). Individually dispersed wood-based cellulose nanocrystals. *ACS*

Applied Materials & Interfaces, 8(9), 5768–5771.
Chevalier, Y., & Bolzinger, M.-A. (2013). Emulsions stabilized with solid nanoparticles: Pickering emulsions. *Colloids and Surfaces A: Physicochemical and Engineering Aspects, 439*, 23–34.
Costa, A. L. R., Gomes, A., Andrade, C. C. P.d., & Cunha, R. L. (2017). Emulsifier functionality and process engineering: Progress and challenges. *Food Hydrocolloids, 68*, 69–80.
Costa, A. L. R., Gomes, A., Tibolla, H., Menegalli, F. C., & Cunha, R. L. (2018). Cellulose nanofibers from banana peels as a Pickering emulsifier: High-energy emulsification processes. *Carbohydrate Polymers, 194*, 122–131.
Costa, A. L. R., Gomes, A., & Cunha, R. L. (2018). One-step ultrasound producing O/W emulsions stabilized by chitosan particles. *Food Research International, 107*, 717–725.
Dapčević Hadnađev, T., Dokić, P., Krstonošić, V., & Hadnađev, M. (2013). Influence of oil phase concentration on droplet size distribution and stability of oil-in-water emulsions. *European Journal of Lipid Science and Technology, 115*(3), 313–321.
Dickinson, E. (1998). Stability and rheological implications of electrostatic milk protein–polysaccharide interactions. *Trends in Food Science & Technology, 9*(10), 347–354.
Dickinson, E., Flint, F. O., & Hunt, J. A. (1989). Bridging flocculation in binary protein stabilized emulsions. *Food Hydrocolloids, 3*(5), 389–397.
Dickinson, E., & Galazka, V. B. (1991). Bridging flocculation in emulsions made with a mixture of protein + polysaccharide. *Food polymers, gels and colloids* (pp. 494–497). Woodhead Publishing.
Domingues, A. A., Pereira, F. V., Sierakowski, M. R., Rojas, O. J., & Petri, D. F. S. (2016). Interfacial properties of cellulose nanoparticles obtained from acid and enzymatic hydrolysis of cellulose. *Cellulose, 23*(4), 2421–2437.
Furtado, G. D. F., Mantovani, R. A., Consoli, L., Hubinger, M. D., & da Cunha, R. L. (2017). Structural and emulsifying properties of sodium caseinate and lactoferrin influenced by ultrasound process. *Food Hydrocolloids, 63*(Supplement C), 178–188.
Furtado, G.d. F., Michelon, M., de Oliveira, D. R. B., & da Cunha, R. L. (2016). Heteroaggregation of lipid droplets coated with sodium caseinate and lactoferrin. *Food Research International, 89*(Part 1), 309–319.
Gomes, A., Costa, A. L. R., & Cunha, R. L. (2018). Impact of oil type and WPI/Tween 80 ratio at the oil-water interface: Adsorption, interfacial rheology and emulsion features. *Colloids and Surfaces B: Biointerfaces, 164*, 272–280.
Gomes, A., Costa, A. L. R., de Assis Perrechil, F., & da Cunha, R. L. (2016). Role of the phases composition on the incorporation of gallic acid in O/W and W/O emulsions. *Journal of Food Engineering, 168*, 205–214.
Goyal, A., Sharma, V., Upadhyay, N., Gill, S., & Sihag, M. (2014). Flax and flaxseed oil: An ancient medicine & modern functional food. *J Food Sci Technol, 51*(9), 1633–1653.
Grishkewich, N., Mohammed, N., Tang, J., & Tam, K. C. (2017). Recent advances in the application of cellulose nanocrystals. *Current Opinion in Colloid & Interface Science, 29*, 32–45. https://doi.org/10.1016/j.cocis.2017.01.005.
Guo, J., Du, W., Gao, Y., Cao, Y., & Yin, Y. (2017). Cellulose nanocrystals as water-in-oil Pickering emulsifiers via intercalative modification. *Colloids and Surfaces A: Physicochemical and Engineering Aspects, 529*, 634–642. https://doi.org/10.1016/j.colsurfa.2017.06.056.
Hedjazi, S., & Razavi, S. H. (2018). A comparison of Canthaxanthine Pickering emulsions, stabilized with cellulose nanocrystals of different origins. *International Journal of Biological Macromolecules, 106*, 489–497.
Horozov, T. S., & Binks, B. P. (2006). Particle-stabilized emulsions: A bilayer or a bridging monolayer? *Angewandte Chemie International Edition, 45*(5), 773–776.
Hu, Z., Ballinger, S., Pelton, R., & Cranston, E. D. (2015). Surfactant-enhanced cellulose nanocrystal Pickering emulsions. *Journal of Colloid and Interface Science, 439*, 139–148.
Hunter, T. N., Pugh, R. J., Franks, G. V., & Jameson, G. J. (2008). The role of particles in stabilising foams and emulsions. *Advances in Colloid and Interface Science, 137*(2), 57–81.
Jafari, S. M., Assadpoor, E., He, Y., & Bhandari, B. (2008). Re-coalescence of emulsion droplets during high-energy emulsification. *Food Hydrocolloids, 22*(7), 1191–1202.
Kalashnikova, I., Bizot, H., Bertoncini, P., Cathala, B., & Capron, I. (2013). Cellulosic nanorods of various aspect ratios for oil in water Pickering emulsions. *Soft Matter, 9*(3), 952–959.
Kalashnikova, I., Bizot, H., Cathala, B., & Capron, I. (2011). New pickering emulsions stabilized by bacterial cellulose nanocrystals. *Langmuir, 27*(12), 7471–7479.
Kalashnikova, I., Bizot, H., Cathala, B., & Capron, I. (2012). Modulation of cellulose nanocrystals amphiphilic properties to stabilize oil/water interface. *Biomacromolecules, 13*(1), 267–275.
Klemm, D., Heublein, B., Fink, H. P., & Bohn, A. (2005). Cellulose: Fascinating biopolymer and sustainable raw material. *Angew Chem Int Ed Engl, 44*(22), 3358–3393.
Lam, E., Male, K. B., Chong, J. H., Leung, A. C. W., & Luong, J. H. T. (2012). Applications of functionalized and nanoparticle-modified nanocrystalline cellulose. *Trends in Biotechnology, 30*(5), 283–290.
Lemarchand, C., Couvreur, P., Vauthier, C., Costantini, D., & Gref, R. (2003). Study of emulsion stabilization by graft copolymers using the optical analyzer Turbiscan. *International Journal of Pharmaceutics, 254*(1), 77–82.
Li, J., Wei, X., Wang, Q., Chen, J., Chang, G., Kong, L., & Liu, Y. (2012). Homogeneous isolation of nanocellulose from sugarcane bagasse by high pressure homogenization. *Carbohydrate Polymers, 90*(4), 1609–1613.
Li, Z., Wu, H., Yang, M., Xu, D., Chen, J., Feng, H., & Kang, W. (2018). Stability mechanism of O/W Pickering emulsions stabilized with regenerated cellulose. *Carbohydrate Polymers, 181*, 224–233.
McClements, D. J. (2005). *Food Emulsions: Principles, practices, and techniques* (2nd ed.). Washington, D.C: CRC Press.
McClements, D. J. (2007). Critical review of techniques and methodologies for characterization of emulsion stability. *Critical Reviews in Food Science and Nutrition, 47*(7), 611–649.
McClements, D. J. (2010). Emulsion design to improve the delivery of functional lipophilic components. In M. P. Doyle, & T. R. Klaenhammer (Vol. Eds.), *Annual review of food science and technology: Vol. 1*, (pp. 241–269). Palo Alto: Annual Reviews.
Mengual, O., Meunier, G., Cayre, I., Puech, K., & Snabre, P. (1999). Characterisation of instability of concentrated dispersions by a new optical analyser: The TURBISCAN MA 1000. *Colloids and Surfaces A: Physicochemical and Engineering Aspects, 152*(1), 111–123.
Mohaiyiddin, M. S., Lin, O. H., Owi, W. T., Chan, C. H., Chia, C. H., Zakaria, S., & Policy, E. (2016). Characterization of nanocellulose recovery from Elaeis guineensis frond for sustainable development. *Clean Technologies and Environmental Policy, 18*(8), 2503–2512.
Naduparambath, S., Jinitha, T. V., Shaniba, V., Sreejith, M. P., Balan, A. K., & Purushothaman, E. (2018). Isolation and characterisation of cellulose nanocrystals from sago seed shells. *Carbohydrate Polymers, 180*(Supplement C), 13–20.
Oguzlu, H., Danumah, C., & Boluk, Y. (2017). Colloidal behavior of aqueous cellulose nanocrystal suspensions. *Current Opinion in Colloid & Interface Science, 29*(Supplement C), 46–56.
Oza, K. P., & Frank, S. G. (1986). Microcrystalline cellulose stabilized emulsions. *Journal of Dispersion Science and Technology, 7*(5), 543–561.
Pang, B., Liu, H., Liu, P., Peng, X., & Zhang, K. (2018). Water-in-oil Pickering emulsions stabilized by stearoylated microcrystalline cellulose. *Journal of Colloid and Interface Science, 513*, 629–637.
Paximada, P., Dimitrakopoulou, E. A., Tsouko, E., Koutinas, A. A., Fasseas, C., & Mandala, I. G. (2016). Structural modification of bacterial cellulose fibrils under ultrasonic irradiation. *Carbohydrate Polymers, 150*, 5–12.
Piorkowski, D. T., & McClements, D. J. (2013). Beverage emulsions: Recent developments in formulation, production, and applications. *FoodHydrocolloids,* 1–37.
Rodriguez-Leyva, D., Bassett, C. M. C., McCullough, R., & Pierce, G. N. (2010). The cardiovascular effects of flaxseed and its omega-3 fatty acid, alpha-linolenic acid. *Canadian Journal of Cardiology, 26*(9), 489–496.
Sanfeld, A., & Steinchen, A. (2008). Emulsions stability, from dilute to dense emulsions — Role of drops deformation. *Advances in Colloid and Interface Science, 140*(1), 1–65.
Santana, R. C., Perrechil, F. A., & Cunha, R. L. (2013). High- and low-energy emulsifications for food applications: A focus on process parameters. *Food Engineering Reviews, 5*(2), 107–122.
Schröder, A., Sprakel, J., Schroën, K., Spaen, J. N., & Berton-Carabin, C. C. (2018). Coalescence stability of Pickering emulsions produced with lipid particles: A microfluidic study. *Journal of Food Engineering, 234*, 63–72.
Segal, L., Creely, J. J., Martin, A. E., & Conrad, C. M. (1959). An empirical method for estimating the degree of crystallinity of native cellulose using the X-ray diffractometer. *Textile Research Journal, 29*(10), 786–794.
Silva, E. K., Gomes, M. T. M. S., Hubinger, M. D., Cunha, R. L., & Meireles, M. A. A. (2015). Ultrasound-assisted formation of annatto seed oil emulsions stabilized by biopolymers. *Food Hydrocolloids, 47*(Supplement C), 1–13.
Silva, E. K., Rosa, M. T. M. G., & Meireles, M. A. A. (2015). Ultrasound-assisted formation of emulsions stabilized by biopolymers. *Current Opinion in Food Science, 5*, 50–59. https://doi.org/10.1016/j.cofs.2015.08.007.
Silva, E. K., Zabot, G. L., Cazarin, C. B. B., Maróstica, M. R., & Meireles, M. A. A. (2016). Biopolymer-prebiotic carbohydrate blends and their effects on the retention of bioactive compounds and maintenance of antioxidant activity. *Carbohydrate Polymers, 144*(Supplement C), 149–158.
Silva, E. K., Zabot, G. L., Toledo Hijo, A. A. C., & Meireles, M. A. A. (2017). Chapter 13 – Encapsulation of bioactive compounds using ultrasonic technology A2 – Bermudez-Aguirre, Daniela. *Ultrasound: Advances for food processing and preservation* (pp. 323–350). Academic Press.
Tang, J., Sisler, J., Grishkewich, N., & Tam, K. C. (2017). Functionalization of cellulose nanocrystals for advanced applications. *Journal of Colloid and Interface Science, 494*(Supplement C), 397–409.
Tang, Y., Yang, S., Zhang, N., & Zhang, J. (2014). Preparation and characterization of nanocrystalline cellulose via low-intensity ultrasonic-assisted sulfuric acid hydrolysis. *Cellulose, 21*(1), 335–346.
Vicentini, N. M., Dupuy, N., Leitzelman, M., Cereda, M. P., & Sobral, P. J. A. (2005). Prediction of cassava starch edible film properties by chemometric analysis of infrared spectra. *Spectroscopy Letters, 38*(6), 749–767.
Wang, H., Wang, J., Qiu, C., Ye, Y., Guo, X., Chen, G., ... Liu, R. H. (2017). Comparison of phytochemical profiles and health benefits in fiber and oil flaxseeds (Linum usitatissimum L.). *Food Chemistry, 214*(Supplement C), 227–233.
Winuprasith, T., & Suphantharika, M. (2013). Microfibrillated cellulose from mangosteen (Garcinia mangostana L.) rind: Preparation, characterization, and evaluation as an emulsion stabilizer. *Food Hydrocolloids, 32*(2), 383–394.
Yuan, Y., & Lee, T. R. (2013). Contact angle and wetting properties. In G. Bracco, & B. Holst (Eds.). *Surface science techniques* (pp. 3–34). Berlin, Heidelberg: Springer, Berlin Heidelberg.